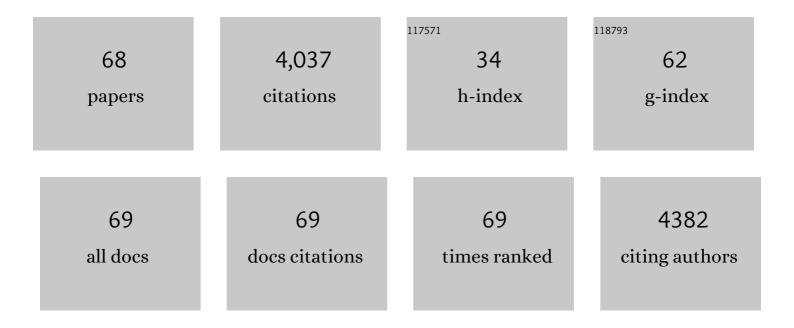
Hui Chen

List of Publications by Year in descending order

Source: https://exaly.com/author-pdf/1011315/publications.pdf Version: 2024-02-01



HUI CHEN

#	Article	IF	CITATIONS
1	Energy level regulation to optimize hydrogen sensing performance of porous bimetallic gallium-indium oxide with ultrathin pore walls. Sensors and Actuators B: Chemical, 2022, 350, 130864.	4.0	6
2	Electronic and morphological dual modulation of NiO by indium-doping for highly improved xylene sensing. New Journal of Chemistry, 2022, 46, 3831-3837.	1.4	8
3	Screening and Understanding Lattice Siliconâ€Controlled Catalytically Active Site Motifs from a Library of Transition Metalâ€6ilicon Intermetallics. Small, 2022, 18, e2107371.	5.2	12
4	Non-catalytic, instant iridium (Ir) leaching: A non-negligible aspect in identifying Ir-based perovskite oxygen-evolving electrocatalysts. Chinese Journal of Catalysis, 2022, 43, 885-893.	6.9	17
5	Light alloying element-regulated noble metal catalysts for energy-related applications. Chinese Journal of Catalysis, 2022, 43, 611-635.	6.9	27
6	Surface-oxidized titanium diboride as cocatalyst on hematite photoanode for solar water splitting. CrystEngComm, 2022, 24, 2251-2257.	1.3	8
7	Metal-Coordinating Single-Boron Sites Confined in Antiperovskite Borides for N ₂ -to-NH ₃ Catalytic Conversion. ACS Catalysis, 2022, 12, 2967-2978.	5.5	11
8	Interfacial engineering of ZIF-67 derived CoSe/Co(OH)2 catalysts for efficient overall water splitting. Composites Part B: Engineering, 2022, 236, 109823.	5.9	22
9	NumericalÂstudyÂonÂcharge transport and electrochemical performance of Gd and Pr co-doped ceria-based solid oxide fuel cells free from internal shorting. Ionics, 2022, 28, 3445-3452.	1.2	4
10	d–sp orbital hybridization: a strategy for activity improvement of transition metal catalysts. Chemical Communications, 2022, 58, 7730-7740.	2.2	37
11	Room temperature, fast fabrication of square meter-sized oxygen evolution electrode toward industrial alkaline electrolyzer. Applied Catalysis B: Environmental, 2022, 316, 121605.	10.8	17
12	Protonated Iridate Nanosheets with a Highly Active and Stable Layered Perovskite Framework for Acidic Oxygen Evolution. ACS Catalysis, 2022, 12, 8658-8666.	5.5	34
13	Crystal phase engineering of electrocatalysts for energy conversions. Nano Research, 2022, 15, 10194-10217.	5.8	13
14	Asymmetrically strained hcp rhodium sublattice stabilized by 1D covalent boron chains as an efficient electrocatalyst. Chemical Communications, 2021, 57, 5075-5078.	2.2	14
15	Olivine-type cadmium germanate: a new sensing semiconductor for the detection of formaldehyde at the ppb level. Inorganic Chemistry Frontiers, 2021, 8, 4467-4473.	3.0	6
16	Design of a Multilayered Oxygenâ€Evolution Electrode with High Catalytic Activity and Corrosion Resistance for Saline Water Splitting. Advanced Functional Materials, 2021, 31, 2101820.	7.8	103
17	Future directions of catalytic chemistry. Pure and Applied Chemistry, 2021, 93, 1411-1421.	0.9	4
18	Iridium-containing water-oxidation catalysts in acidic electrolyte. Chinese Journal of Catalysis, 2021, 42, 1054-1077.	6.9	66

Ниі Снем

#	Article	IF	CITATIONS
19	Pt-decorated foam-like Ga-In bimetal oxide nanofibers for trace acetone detection in exhaled breath. Journal of Alloys and Compounds, 2021, 873, 159813.	2.8	9
20	Realization of interstitial boron ordering and optimal near-surface electronic structure in Pd-B alloy electrocatalysts. Chemical Engineering Journal, 2021, 419, 129568.	6.6	23
21	High-performance formaldehyde sensing realized by alkaline-earth metals doped In2O3 nanotubes with optimized surface properties. Sensors and Actuators B: Chemical, 2020, 304, 127241.	4.0	38
22	Transitionâ€Metal–Boron Intermetallics with Strong Interatomic d–sp Orbital Hybridization for Highâ€Performance Electrocatalysis. Angewandte Chemie, 2020, 132, 3989-3993.	1.6	88
23	Theoretical insights into nonprecious oxygen-evolution active sites in Ti–Ir-Based perovskite solid solution electrocatalysts. Journal of Materials Chemistry A, 2020, 8, 218-223.	5.2	15
24	Transitionâ€Metal–Boron Intermetallics with Strong Interatomic d–sp Orbital Hybridization for Highâ€Performance Electrocatalysis. Angewandte Chemie - International Edition, 2020, 59, 3961-3965.	7.2	139
25	Multiple crystal phases of intermetallic tungsten borides and phase-dependent electrocatalytic property for hydrogen evolution. Chemical Communications, 2020, 56, 13983-13986.	2.2	32
26	Low-iridium electrocatalysts for acidic oxygen evolution. Dalton Transactions, 2020, 49, 15568-15573.	1.6	19
27	Active Site Engineering in Porous Electrocatalysts. Advanced Materials, 2020, 32, e2002435.	11.1	304
28	Perovskiteâ€īype Solid Solution Nanoâ€Electrocatalysts Enable Simultaneously Enhanced Activity and Stability for Oxygen Evolution. Advanced Materials, 2020, 32, e2001430.	11.1	107
29	Optimization of Active Sites via Crystal Phase, Composition, and Morphology for Efficient Lowâ€ŀridium Oxygen Evolution Catalysts. Angewandte Chemie - International Edition, 2020, 59, 19654-19658.	7.2	79
30	Optimization of Active Sites via Crystal Phase, Composition, and Morphology for Efficient Lowâ€Iridium Oxygen Evolution Catalysts. Angewandte Chemie, 2020, 132, 19822-19826.	1.6	11
31	Intermetallic borides: structures, synthesis and applications in electrocatalysis. Inorganic Chemistry Frontiers, 2020, 7, 2248-2264.	3.0	94
32	Alkali metal-incorporated spinel oxide nanofibers enable high performance detection of formaldehyde at ppb level. Journal of Hazardous Materials, 2020, 400, 123301.	6.5	33
33	Crystal phase-dependent electrocatalytic hydrogen evolution performance of ruthenium–boron intermetallics. Chemical Communications, 2020, 56, 3061-3064.	2.2	44
34	Identifying Key Structural Subunits and Their Synergism in Low-Iridium Triple Perovskites for Oxygen Evolution in Acidic Media. Chemistry of Materials, 2020, 32, 3904-3910.	3.2	29
35	Revealing Activity Trends of Metal Diborides Toward pHâ€Universal Hydrogen Evolution Electrocatalysts with Ptâ€Like Activity. Advanced Energy Materials, 2019, 9, 1803369.	10.2	111
36	Enhanced Iridium Mass Activity of 6H-Phase, Ir-Based Perovskite with Nonprecious Incorporation for Acidic Oxygen Evolution Electrocatalysis. ACS Applied Materials & Interfaces, 2019, 11, 42006-42013.	4.0	48

Ниі Снем

#	Article	IF	CITATIONS
37	High-performance oxygen evolution electrocatalysis by boronized metal sheets with self-functionalized surfaces. Energy and Environmental Science, 2019, 12, 684-692.	15.6	169
38	Promoting Subordinate, Efficient Ruthenium Sites with Interstitial Silicon for Pt‣ike Electrocatalytic Activity. Angewandte Chemie, 2019, 131, 11531-11535.	1.6	92
39	A class of metal diboride electrocatalysts synthesized by a molten salt-assisted reaction for the hydrogen evolution reaction. Chemical Communications, 2019, 55, 8627-8630.	2.2	57
40	Promoting Subordinate, Efficient Ruthenium Sites with Interstitial Silicon for Pt‣ike Electrocatalytic Activity. Angewandte Chemie - International Edition, 2019, 58, 11409-11413.	7.2	128
41	Tailoring energy level and surface basicity of metal oxide semiconductors by rare-earth incorporation for high-performance formaldehyde detection. Inorganic Chemistry Frontiers, 2019, 6, 1767-1774.	3.0	25
42	Activating Inert, Nonprecious Perovskites with Iridium Dopants for Efficient Oxygen Evolution Reaction under Acidic Conditions. Angewandte Chemie, 2019, 131, 7713-7717.	1.6	123
43	<i>In situ</i> structural evolution of a nickel boride catalyst: synergistic geometric and electronic optimization for the oxygen evolution reaction. Journal of Materials Chemistry A, 2019, 7, 5288-5294.	5.2	69
44	Activating Inert, Nonprecious Perovskites with Iridium Dopants for Efficient Oxygen Evolution Reaction under Acidic Conditions. Angewandte Chemie - International Edition, 2019, 58, 7631-7635.	7.2	176
45	Surface-clean, phase-pure multi-metallic carbides for efficient electrocatalytic hydrogen evolution reaction. Inorganic Chemistry Frontiers, 2019, 6, 940-947.	3.0	29
46	Enhanced sensing performance to toluene and xylene by constructing NiGa2O4-NiO heterostructures. Sensors and Actuators B: Chemical, 2019, 282, 331-338.	4.0	51
47	Well-Tuned Surface Oxygen Chemistry of Cation Off-Stoichiometric Spinel Oxides for Highly Selective and Sensitive Formaldehyde Detection. Chemistry of Materials, 2018, 30, 2018-2027.	3.2	64
48	Oxygen vacancy-rich, Ru-doped In ₂ O ₃ ultrathin nanosheets for efficient detection of xylene at low temperature. Journal of Materials Chemistry C, 2018, 6, 4156-4162.	2.7	42
49	Enhanced formaldehyde sensing properties of IrO2-loaded porous foam-like Ga1.4In0.6O3 nanofibers with ultrathin pore walls. Journal of Alloys and Compounds, 2018, 732, 856-862.	2.8	6
50	Enhanced Electrochemical Activity and Chromium Tolerance of the Nucleation-Agent-Free La2Ni0.9Fe0.1O4+l´Cathode by Gd0.1Ce0.9O1.95 Incorporation. Electronic Materials Letters, 2018, 14, 432-439.	1.0	6
51	Revealing the Relationship between Energy Level and Gas Sensing Performance in Heteroatom-Doped Semiconducting Nanostructures. ACS Applied Materials & Interfaces, 2018, 10, 29795-29804.	4.0	74
52	Porous Ga–In Bimetallic Oxide Nanofibers with Controllable Structures for Ultrasensitive and Selective Detection of Formaldehyde. ACS Applied Materials & Interfaces, 2017, 9, 4692-4700.	4.0	95
53	Accelerated room-temperature crystallization of ultrahigh-surface-area porous anatase titania by storing photogenerated electrons. Chemical Communications, 2017, 53, 1619-1621.	2.2	19
54	Ultrathin In ₂ O ₃ Nanosheets with Uniform Mesopores for Highly Sensitive Nitric Oxide Detection. ACS Applied Materials & Interfaces, 2017, 9, 16335-16342.	4.0	108

Hui Chen

#	Article	IF	CITATIONS
55	Effects of impact energy on the wear resistance and work hardening mechanism of medium manganese austenitic steel. Friction, 2017, 5, 447-454.	3.4	20
56	Electrospinning preparation of mesoporous spinel gallate (MGa2O4; M Ni, Cu, Co) nanofibers and their M(II) ions-dependent gas sensing properties. Sensors and Actuators B: Chemical, 2017, 240, 689-696.	4.0	46
57	Electrospinning Synthesis of Bimetallic Nickel–Iron Oxide/Carbon Composite Nanofibers for Efficient Water Oxidation Electrocatalysis. ChemCatChem, 2016, 8, 992-1000.	1.8	69
58	Unique Electronic Structure in a Porous Gaâ€In Bimetallic Oxide Nanoâ€Photocatalyst with Atomically Thin Pore Walls. Angewandte Chemie, 2016, 128, 11614-11618.	1.6	5
59	Unique Electronic Structure in a Porous Gaâ€In Bimetallic Oxide Nanoâ€Photocatalyst with Atomically Thin Pore Walls. Angewandte Chemie - International Edition, 2016, 55, 11442-11446.	7.2	40
60	Graphene-nanosheet-wrapped LiV3O8 nanocomposites as high performance cathode materials for rechargeable lithium-ion batteries. Journal of Power Sources, 2016, 307, 426-434.	4.0	38
61	Metallic Co ₉ S ₈ nanosheets grown on carbon cloth as efficient binder-free electrocatalysts for the hydrogen evolution reaction in neutral media. Journal of Materials Chemistry A, 2016, 4, 6860-6867.	5.2	265
62	Precursor-mediated synthesis of double-shelled V ₂ O ₅ hollow nanospheres as cathode material for lithium-ion batteries. CrystEngComm, 2016, 18, 4068-4073.	1.3	21
63	Carbon-Armored Co ₉ S ₈ Nanoparticles as All-pH Efficient and Durable H ₂ -Evolving Electrocatalysts. ACS Applied Materials & Interfaces, 2015, 7, 980-988.	4.0	335
64	Growth of molybdenum carbide micro-islands on carbon cloth toward binder-free cathodes for efficient hydrogen evolution reaction. Journal of Materials Chemistry A, 2015, 3, 16320-16326.	5.2	100
65	A high surface area flower-like Ni–Fe layered double hydroxide for electrocatalytic water oxidation reaction. Dalton Transactions, 2015, 44, 11592-11600.	1.6	90
66	Enhanced electrochemical performance of Li3V2(PO4)3 microspheres assembled with nanoparticles embedded in a carbon matrix. RSC Advances, 2015, 5, 31410-31414.	1.7	9
67	Synthesis of porous In ₂ O ₃ microspheres as a sensitive material for early warning of hydrocarbon explosions. RSC Advances, 2015, 5, 5424-5431.	1.7	28
68	Crystal phase-selective synthesis of intermetallic palladium borides and phase-regulated (electro)catalytic properties. Catalysis Science and Technology, 0, , .	2.1	6